



Transfer of orbital angular momentum on a macroscopic object in the UHF frequency band

Ronan Niemiec, Christian Brousseau, Olivier Emile, Kouroch Mahdjoubi

► To cite this version:

Ronan Niemiec, Christian Brousseau, Olivier Emile, Kouroch Mahdjoubi. Transfer of orbital angular momentum on a macroscopic object in the UHF frequency band. AES2012 - Advanced Electromagnetics Symposium, Apr 2012, Paris, France. pp.1. hal-00776494

HAL Id: hal-00776494

<https://hal.science/hal-00776494>

Submitted on 15 Jan 2013

HAL is a multi-disciplinary open access archive for the deposit and dissemination of scientific research documents, whether they are published or not. The documents may come from teaching and research institutions in France or abroad, or from public or private research centers.

L'archive ouverte pluridisciplinaire **HAL**, est destinée au dépôt et à la diffusion de documents scientifiques de niveau recherche, publiés ou non, émanant des établissements d'enseignement et de recherche français ou étrangers, des laboratoires publics ou privés.

Transfer of orbital angular momentum on macroscopic object in the UHF band

Ronan Niemiec^{1,2}, Christian Brousseau¹, Olivier Emile²,
and Kouroch Mahdjoubi¹

¹UMR 6164 IETR, Université de Rennes 1, 35042 Rennes Cedex, France

²URU 435 Physique des Lasers, Université de Rennes 1, 35042 Rennes Cedex, France

*corresponding author, E-mail: ronan.niemiec@univ-rennes1.fr

Abstract

We report on the exchange of orbital angular momentum between an electromagnetic microwave and a macroscopic object. Using a quadrupole wire antenna at frequency $f = 870 \text{ MHz}$, we induce a torque on a suspended copper strip. The induced torque on the strip is of the order of 10^{-8} Nm . A linear dependence of the acceleration of the strip on the radiated power, up to $8 \cdot 10^{-4} \text{ \%s}^2$, is observed and rotations of a few degrees are measured.

1. Introduction

An electromagnetic (EM) wave is defined by its magnitude, its wave vector, its frequency and its angular momentum. Angular momentum is the mechanical property of an EM wave and can be decomposed in two components:

- The intrinsic component which is the Spin Angular Momentum (SAM), associated to the wave polarization,
- The extrinsic part which is the Orbital Angular Momentum (OAM), which represents the spatial distribution and depends on the gradient of the EM fields.

Since the pioneering experiment of Beth in 1935 [1], it is well known that the circular polarization of EM waves can induce rotation of macroscopic birefringent plates. This effect has since been experimentally confirmed either at macroscopic scale, both in optics [1, 2] and microwaves [3, 4], or at microscopic scales [5] in optics only. In 1949, Carrara [3] measured rotations of few degrees of various absorbing macroscopic objects, like 3cm size-disks and squares, using circularly polarized waves at a frequency of 9.36 GHz with a mean power of 50 W . More refining experiments have been conducted by Allen in 1966 [4], at a frequency of 9.3 GHz . Continuous rotation of a small dipole, delicately suspended in a circular waveguide, has been observed using an incident circular polarized wave of low power (less than 1 W).

On the other hand, according to the Maxwell equations, electromagnetic fields can also carry orbital angular momentum (OAM) when the wavefronts are twisted

regarded to the direction of propagation. In 1992, Allen *et al.* [6] showed that light beams with an azimuthal phase dependence $\exp(i.l.\varphi)$, carry an orbital angular momentum of $l.\hbar$ per photon, where \hbar is the reduced Planck constant, and l , an integer number called the “topological charge” [7]. From these studies, an analogous adventure can be considered for the orbital angular momentum (OAM) of an EM field to rotate objects. Indeed, transfer of OAM has already been observed on microparticles [8]. However, in the macroscopic domain, no direct evidence of OAM transfer from an EM wave has ever been observed. Besides, in the microwave or in the radiofrequency domain, such an effect would be easier to evidence since the angular momentum carried by the EM wave could be much higher for a given power. For example in Carrara’s experiment [3], the induced torque was indeed observed with the naked eyes.

In this paper, we report the experimental observation of the OAM transfer from an EM wave to a macroscopic object suspended by a torsion pendulum, in the radiofrequency domain. In a first part, the experimental setup is described and characterized. In a second part, experimental results are presented and discussed. Finally, a conclusion is presented and some improvements are proposed.

2. Experimental Setup

In 1987, Vul’fson [9] proposed an experimental setup to measure the angular momentum of EM radiation with a wavelength of the order of $1\text{-}1.5 \text{ cm}$, using a torsion pendulum. However, such an experimental setup has not been realized yet.

Torsion pendulum is a very popular tool that has been used for over more than two centuries for fundamental measurements [10, 11] and is still the most sensitive tool for measuring weak torques. It has also been used in photon spin angular momentum transfer to a macroscopic object [1-4]. The schematic diagram we used to measure angular momentum in the UHF range is presented in Fig.1 showing in particular the suspended receiving ring, which is the detector of the angular momentum.

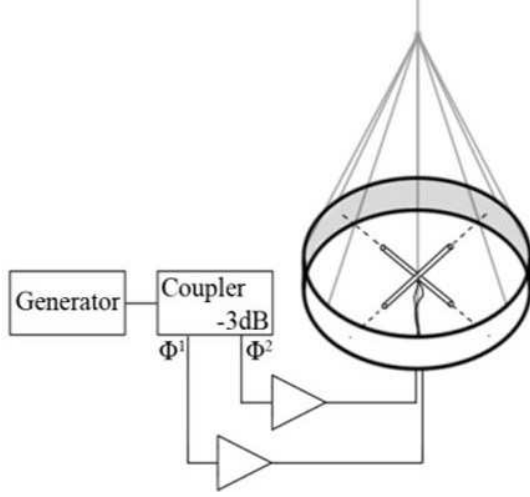


Figure 1: Schematic diagram of the experimental set-up, as inspired from Vul'son's proposal [9], showing the RF frequency generator, the -3dB coupler, the power amplifiers, the antennas and the copper detector ring.

This experimental system is composed of:

- a RF frequency signal synthesizer (Generator),
- a -3 dB coupler,
- two power amplifiers,
- two dipole antennas.

Orbital angular momentum is detected by a light copper ring which has the following dimensions:

- internal radius R_i : 15.4 cm ,
- height h_r : 5 cm ,
- thickness: $156\text{ }\mu\text{m}$.

From these parameters, the inertial momentum J can be determined using the following equation:

$$J = \frac{1}{2} \cdot M \cdot (R_2^2 + R_1^2), \quad (1)$$

where:

$$M = \rho \cdot \pi \cdot h_r \cdot (R_2^2 - R_1^2), \quad (2)$$

Where R_i and R_2 are respectively the internal and the external radius of the ring, h_r , the height of the ring, and ρ , the copper density equals to 8.94 g.cm^{-3} . Therefore, the inertial momentum is evaluated to be $J = 8.4 \cdot 10^{-4}\text{ kg.m}^2$.

The ring is suspended to the ceiling of the room with an ordinary cotton thread. This thread has a length of 2 m and a diameter of 0.5 mm . It is then attached to the ring by eight branches of cotton thread. The torsion constant of this suspension has been then deduced from the 12 min period of the free oscillation of the pendulum and equals to $\Gamma = 6.26 \cdot 10^{-8}\text{ Nm}^\circ$.

From Fig.2, one can see the two dipole antennas at the center of the ring, which are orthogonal to each other. These antennas are supplied from a common frequency synthesizer with a phase shift of $\pm \pi/2$. These two dipole antennas are made from a copper wire that has a diameter of 2 mm and a length of 17 cm .

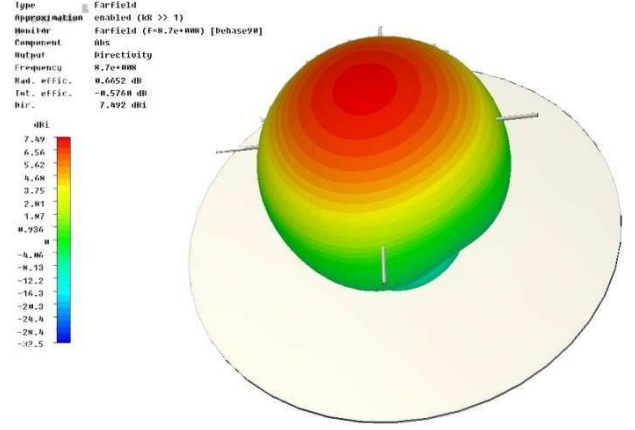


Figure 2: 3D radiation pattern of the two crossed dipole antennas in the far field, at the frequency of $f = 870\text{ MHz}$.

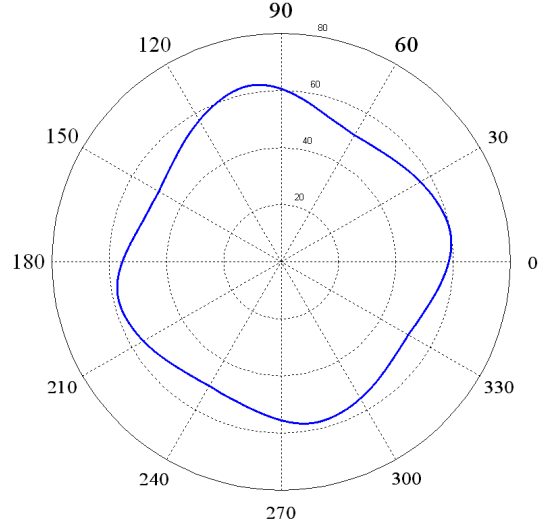


Figure 3: Electrical field radiated by a turnstile antenna composed of two crossed dipoles excited in phase quadrature, at the distance of 15.4 cm . Transmitted power is equal to 1 W . The field is calculated at the frequency of $f = 870\text{ MHz}$ and in the plane of antennas. Pattern dissymmetrical defect is due to a small difference on the size of the realized dipoles.

This type of antenna is known as turnstile antenna, whose principal characteristic is an isotropic radiation pattern. Thus, the electric field is constant all over the copper ring, ensuring a global symmetry of the system [12].

Fig.2 and Fig.3 present, respectively, the 3D radiation pattern and the E field radiated by the turnstile antenna in the far field. The latter is calculated in the plane of antennas, at a distance of 15.4 cm to the center and at a frequency of 870 MHz . These results are computed using CST numerical electromagnetic software. Small variations are observed along the radiation pattern due to a small difference on the antenna size.

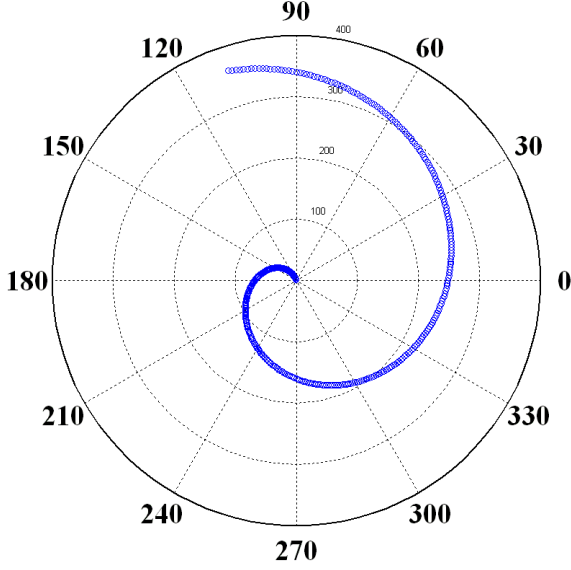


Figure 4: Phase variation of the radiated EM field as a function of the azimuth angle (Φ angle), in the plane of antennas and at the frequency of 870 MHz.

The measured SWR is around 1.3 for each antenna. These antennas, having a power supply with a $\pi/2$ phase shift, are often used for circular polarization applications (e.g. satellite communications), because the far field radiation pattern in front of the antennas has a circular polarization. The turnstile antenna is also used in broadcast applications, where there is a need for horizontal (linear) polarization with uniform (isotropic) radiation pattern around the antenna. However, in our case, we are interested in the EM field in the plane of the antennas only.

In the near field and in the plane of the antennas, the radiated electromagnetic field is near-isotropic (Fig.3) and has a 2π phase rotation as a function of the azimuth angle (Φ angle). This is in fact, the characteristic behavior of an EM wave carrying an orbital angular momentum with a topological charge l equal to $l=1$ (Fig. 4).

These dipoles are supplied from a CW (Continuous Wave) frequency synthesizer through a -3 dB coupler (power divider) having a $\pi/2$ phase shift. A picture of this -3 dB power-divider/phase-shifter is shown in Fig.5. Then, the RF signals, which are now in phase quadrature, are amplified by two 40 dB gain power amplifiers before being supplied to the antennas, through 2 coaxial cables of 5 m long.

Finally, the gain and phase induced by the electronic parts (amplifiers, cables, connectors, ...) between the output of the RF frequency synthesizer and the inputs of each antenna, have been measured using a vector network analyzer. Measurements are summarized in Table 1. Gains of the two transmission lines (TL1 and TL2) are very close to each other, with a difference of 0.8 dB. The phase difference is equal to 85.8°, which is slightly smaller than the desired 90°, despite the difference of lengths of the two output ports of the -3 dB coupler. But, we will see in the next part that it is good enough for our experiment.

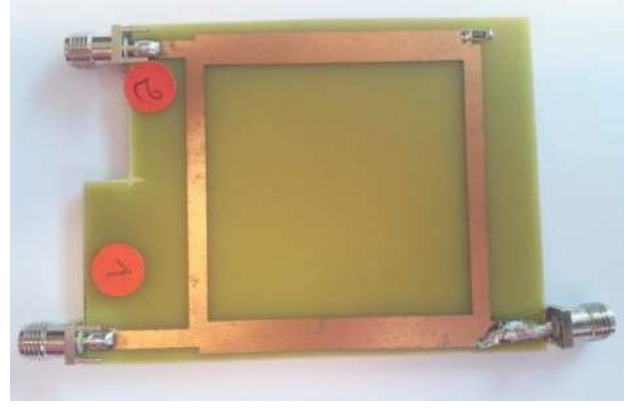


Figure 5: Picture of the -3 dB coupler/power divider with a $\pi/2$ phase shift between outputs 1 and 2. The output port 2 is slightly shorter than port 1 to compensate for the phase discrepancy between the transmission lines (amplifiers + coaxial cables) used to feed the dipole antennas

Table 1: Gain and phase introduced by the electronic parts between the output of the RF frequency synthesizer and the inputs of the antenna 1 (TL1) and the antenna 2 (TL2).

	TL1	TL2
Gain (dB)	39.8	40.6
Phase (deg.)	178.6	-95.6

Special care has been taken to avoid spurious effects. The experimental setup is confined in an anechoic chamber. Besides, the suspension and the experimental setup have been isolated from any mechanical vibration. Rotation of the ring is recorded via a webcam connected to a computer located outside of the anechoic chamber. Fig.6 and Fig.7 show pictures of the experimental setup placed in the anechoic chamber.

3. Fields

The electric field radiated by one dipole antenna alone writes in the far field:

$$E_{\theta,1} = \frac{L}{4.\epsilon_0.c.\lambda} \cdot \frac{\cos\left(\frac{\pi}{2} \cdot \cos\theta\right)}{r \cdot \sin\theta} \cdot I_0 \cdot e^{j(\omega t - kr)} \quad , \quad (3)$$

$$E_{\theta,1} \approx \frac{L}{4.\epsilon_0.c.\lambda} \cdot \frac{\sin(\theta)}{r} \cdot I_0 \cdot e^{j(\omega t - kr)}$$

where λ is the wavelength of the electric field, k , the wave vector, L , the length of the antenna, c , the velocity of light, ϵ_0 , the dielectric constant, ω , the angular frequency of the current in the dipole, I_0 , its amplitude, (r, θ) , the usual polar coordinates, and j is the usual complex number. Note that the estimated electric field lies in the plane of the antennas and is thus tangential to the copper ring.



Figure 6: Picture of the experimental set-up showing the suspended detector ring in the anechoic chamber.

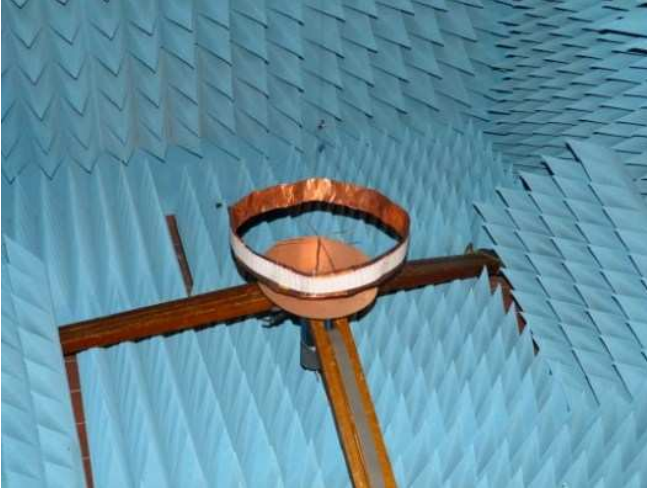


Figure 7: Experimental set-up showing the antennas and the suspended ring in the anechoic chamber.

Since there is a phase of $\phi = \pi/2$ to the signal sent to the second antenna, its radiated electric field can be written:

$$E_{\theta,2} \approx \frac{L}{4.\epsilon_0.c.\lambda} \cdot \frac{\cos(\theta)}{r} \cdot I_0 \cdot e^{j\left(\omega t - kr - \frac{\pi}{2}\right)}, \quad (4)$$

This leads to a total electric field which also lies in the plane of the antennas:

$$E_{\theta} \approx \frac{-j}{r} \cdot e^{j.\theta} \frac{L}{4.\epsilon_0.c.\lambda} \cdot I_0 \cdot e^{j.(\omega t - kr)}, \quad (5)$$

Note the phase factor $\exp(j\theta)$ in this expression. Actually, this factor leads to a spatial modulation of the phase of the

field. In such an electric field, the phase fronts are twisted and the orbital momentum is \hbar per photon.

4. Measurements

The antennas have been excited with powers, varying from 1.5 W up to 25 W . The corresponding rotation of the pendulum has been recorded and is displayed as a function of time on Fig. 8. For the sake of clarity, the rotations for four radiated powers (3 W , 6 W , 8 W and 25 W) have been plotted with a fit of the experimental data with parabolas.

As one can see, the rotation of the pendulum is a uniformly accelerated rotation within a very good approximation. To our knowledge, it is the first direct observation of the transfer of electromagnetic orbital angular momentum to a macroscopic object. For a longer time of observation, the restoring torque of the thread becomes no longer negligible and this leads to damped oscillations. As expected, the rotation becomes more important as the power is increased. An inversion of the rotation of the pendulum is also experimentally observed for a reversing of the phase shift from $+\pi/2$ to $-\pi/2$. This is equivalent to remove the minus sign just in front of θ in Eq. 5. Thus, it corresponds to the change from $+\hbar$ to $-\hbar$ OAM carried per photon. Then, the sign of the torque should also be reversed as we can see in Fig. 8.

Besides, we can also observe in Fig. 8, that the two recordings of the rotation for both directions are nearly perfectly symmetric.

Finally, when the two dipoles are in phase ($\phi = 0$), no rotation is observed, meaning that parasitic effects such as, radiation pressure due to a misalignment of the pendulum regarding the antennas, or reflection from the walls or the ground of the chamber, are negligible in our experimental setup.

Based on the measurement of the angle of rotation as a function of time reported in Fig. 8, angular acceleration transferred by the electric field to the strip as a function of the applied power has been estimated. Since the applied torque is \hbar per photon, the total torque should be proportional to the number of photons, and thus the angular acceleration should depends linearly on the applied power. Indeed, the experimental results show a nearly perfect linear dependence on the applied power. Moreover, the linear dependence holds over more than one order of magnitude, from 1.5 W to 25 W .

The symmetry between both directions of rotation is also verified. The linear coefficient deduced from the fitting of the experimental data is exactly the inverse for one direction of rotation and for the other direction.

From Fig. 8, for a power of 25 W , we can deduce an angular acceleration of $a = 6.4 \times 10^{-4} \text{ }^\circ/\text{s}^2$.

This corresponds to an applied torque Γ applied to the ring by the EM microwave radiation due to the OAM:

$$\Gamma = J.a = 4.71 \times 10^{-9} \text{ Nm} \quad (6)$$

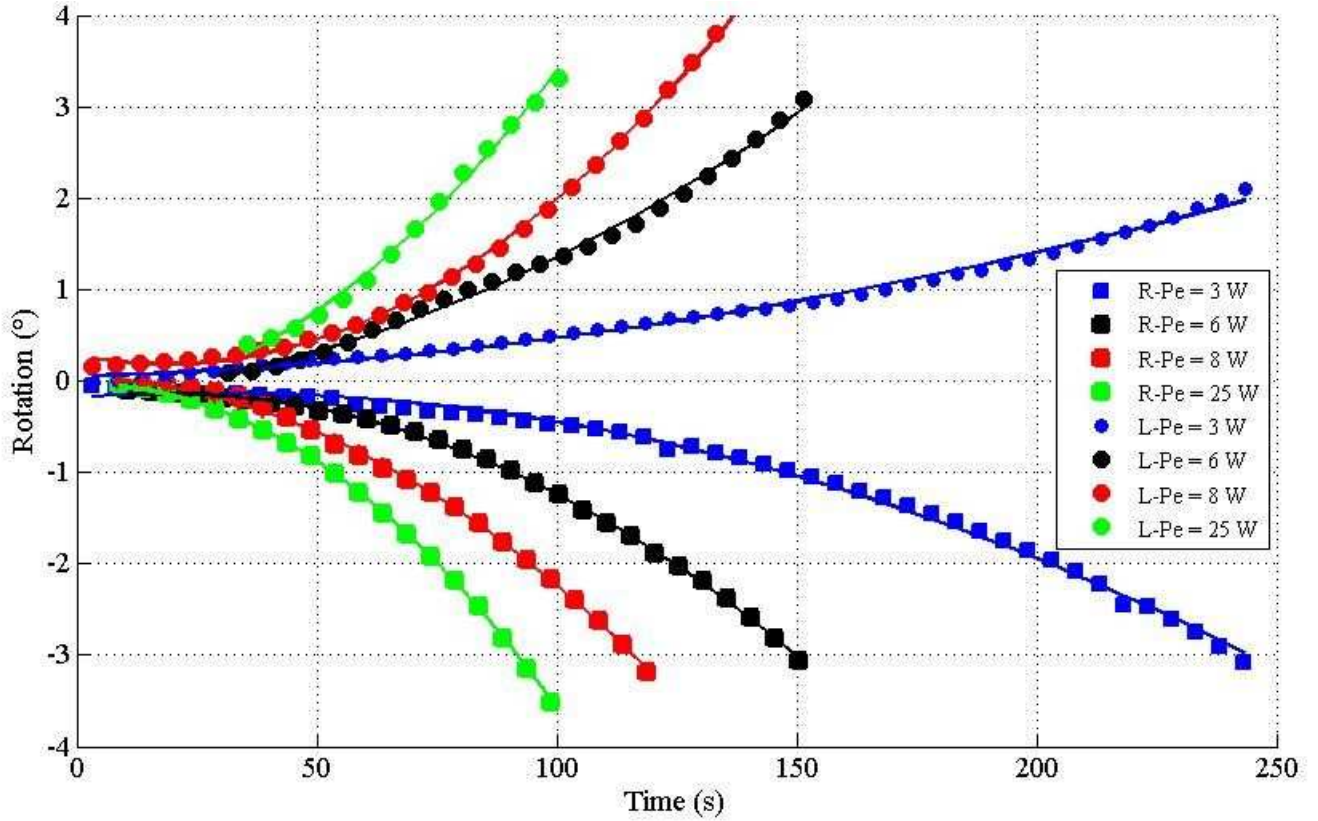


Figure 8: Angular rotation as a function of time for a $-\pi/2$ (“R”curves) and $+\pi/2$ (“L”curves) phase shift between the antennas and for different transmitted powers P_e (3 W, 6 W, 8 W and 25 W).

5. Discussions

Thanks to the very high sensitivity of the torsion pendulum, we have been able to detect an applied torque of the order of $\Gamma = 10^{-9} \text{ Nm}$ due to the transfer of orbital angular momentum of the photon. By improving the suspension mechanism, as well as the thread suspension [13], like using spider draglines, and by inserting the experimental setup in a vacuum chamber to reduce the damping coefficient, a detection of a torque of the order of $\Gamma = 10^{-14} \text{ Nm}$ seems within reach. The absorbing object could be either an absorbing ring or strip in the case a spherical wave, or an adapted absorbing plate in the case of a plane wave. This would correspond to electromagnetic fields carrying orbital angular momentum in the microwatt range or lower. This may be an alternative way to detect orbital angular momentum in the radio domain [14, 15] or even in astronomy [16].

6. Conclusions

To conclude, we have experimentally observed the transfer of angular orbital momentum from an electromagnetic wave to a macroscopic object using a torsion pendulum, at the frequency of 870 MHz.

A microwave field has been generated using a linear quadrupole antenna (turnstile antenna) with a controlled dephasing between the antennas. A phase rotation of 2π is observed on this electromagnetic field, in the plane of the antennas, characteristic phenomenon of a EM field carrying an angular orbital momentum of \hbar per photon. The accelerating regime of the pendulum has been isolated and it is possible to switch the direction of the rotation simply by inverting the phase shift between the two dipole antennas. It would be now stimulating to try to detect microwave electromagnetic field carrying more than one \hbar per photon.

Acknowledgements

We would like to thank K. Wang, T. Teko, and A. Adibi for early interest, and D. Levalois and R. Legave for technical assistance. This work was supported by the University of Rennes 1 via a “défi émergent” action, the French Ministry of Defense (DGA) and the council of Brittany (Région Bretagne).

References

- [1] R.A. Beth, Mechanical detection and measurement of the angular momentum of light, *Physical Review*, 50: 115–125, 1936.

- [2] G. Delannoy, O. Emile, A. Le Floch, Direct observation of a photon spin-induced constant acceleration in macroscopic systems, *Applied Physical Letters*, 86: 081109, 2005.
- [3] N. Carrara, Torque and angular momentum of centimetre electromagnetic waves, *Nature*, 164: 882–884, 1949.
- [4] P.J. Allen, A radiation torque experiment, *American Journal of Physics*, 34: 1185–1192, 1966.
- [5] M.E.J. Friese, T.A. Nieminen, N.R. Heckenberg, H. Rubinsztein-Dunlop, Optical alignment and spinning of laser-trapped microscopic particles, *Nature*, 394: 348–350, 1998.
- [6] L. Allen, M.W. Beijersbergen, R.J.C. Spreeuw, J.P. Woerdman, Orbital angular momentum of light and the transformation of Laguerre-Gaussian laser modes, *Physical Review A*, 45: 8185–8189, 1992.
- [7] M. Padgett, R. Bowman, Tweezers with a twist, *Nature Photonics* 5: 343–348, 2011.
- [8] H. He, M.E.J. Friese, N.R. Heckenberg, H. Rubinsztein-Dunlop, Direct observation of transfer of angular momentum to absorptive particles from a laser beam with a phase singularity, *Physical Review Letters*, 75: 826–829, 1995.
- [9] K.S. Vul’fson, Angular momentum of electromagnetic waves, *Soviet Physics Uspekhi*, 30 (8), pp. 724–728, August 1988.
- [10] H. Cavendish, Experiments to determine the density of earth, *Philosophical Transactions of the Royal Society*, London 8: 469, 1798.
- [11] C.A. Coulomb, *Mémoires de Coulomb*, édité par les soins d’A. Potier, Imprimeur Gauthier-Villars, Paris 1884.
- [12] S.G.M. Darwish, K.F.A. Hussein, H.A. Mansour, Circularly polarized crossed-dipole turnstile antenna for satellites, *Proceedings of the Twenty-First NRSC2004 - National Radio Science Conference*, June 2004, Monterey, California, USA.
- [13] O. Emile, A. Le Floch, A. Vollrath, Time-resolved Torsional relaxation of spider draglines by an optical technique, *Physical Review Letters*, 98: 167402, 2007.
- [14] H. The, B. Thidé, J.T. Mendonça, T.D. Carozzi, J. Bergman, W.A. Baan, S. Mohammadi, B. Eliasson, Detecting orbital angular momentum in radio signals, *arXiv.org*, astro-ph(0805.2735), 18 May 2008, <http://arxiv.org/abs/0805.2735>.
- [15] S.M. Mohammadi, L.K.S. Daldorff, R.L. Karlsson, B. Thidé, K. Forozesh, T.D. Carozzi, and B. Isham, Orbital angular momentum in radio - A system study, *IEEE Transactions on Antennas and Propagation*, 58: 565, 2010.
- [16] N.M. Elias, Photon orbital momentum in astronomy, *Astronomy & Astrophysics*, 492: 883, 2008.